HHS Public Access

Author manuscript

*Curr Pharm Des*. Author manuscript; available in PMC 2016 October 02.

Published in final edited form as:

*Curr Pharm Des*. 2012 ; 18(15): 2152–2165.

# Phase-Change Contrast Agents for Imaging and Therapy

**Paul S. Sheeran** and **Paul A. Dayton***

Joint Department of Biomedical Engineering, The University of North Carolina and North Carolina State University, Chapel Hill, NC, 27599

## Abstract

Phase-change contrast agents (PCCAs) for ultrasound-based applications have resulted in novel ways of approaching diagnostic and therapeutic techniques beyond what is possible with microbubble contrast agents and liquid emulsions. When subjected to sufficient pressures delivered by an ultrasound transducer, stabilized droplets undergo a phase-transition to the gaseous state and a volumetric expansion occurs. This phenomenon, termed acoustic droplet vaporization, has been proposed as a means to address a number of *in vivo* applications at the microscale and nanoscale. In this review, the history of PCCAs, physical mechanisms involved, and proposed applications are discussed with a summary of studies demonstrated *in vivo*. Factors that influence the design of PCCAs are discussed, as well as the need for future studies to characterize potential bioeffects for administration in humans and optimization of ultrasound parameters.

### Keywords

ultrasound; contrast agent; phase-change; acoustic droplet vaporization; perfluorocarbon; microbubble; drug delivery; diagnostic imaging

## INTRODUCTION

The relatively recent concept of designing diagnostic and therapeutic phase-change contrast agents (PCCAs) based on an ultrasound triggered phase-transition has provided medical researchers with a ‘middle-ground’ between the inert liquid emulsion and gas-based microbubble contrast agent (MCA) platforms. PCCAs can be generated in a wide range of useful sizes and, once activated, show high echogenicity (Fig. **1**). The ability to ultrasonically induce activation with temporal and spatial specificity has resulted in the emergence of a diverse set of techniques for *in vivo* and *in vitro* applications.

Perfluorochemicals and perfluorocarbons (referred to collectively here as PFCs), in both the liquid and gaseous state, have proven to be favorable compounds for inert liquid emulsions, MCAs, and PCCAs due to their unique properties. When administered *in-vivo*, liquid emulsions of high boiling-point PFCs are inert, non-toxic in small doses, and can have relative stability in circulation due to high molecular weight, immiscibility in water, and low surface tension [1, 2]. Depending on the choice of PFC, the emulsions may persist stably *in-*

*Corresponding Author, padayton@bme.unc.edu, Address: 304 Taylor Hall, CB 7575, Chapel Hill, NC 27599, Phone: (919) 843-9521, Fax: (919) 843-9520.

*vivo* for hours to days [3], which is attractive for applications involving gradual accumulation at a target site and/or sustained release of drugs. Applications are not strictly intra-vascular because liquid PFC emulsions can be generated with a broad range of sizes, including the hundred-nanometer range. A number of applications have been proposed, including molecular imaging and therapy of thrombi, tumor angiogenesis, and atherosclerosis-related diseases [4–8], quantitative *in vivo* imaging and contrast enhancement [1, 3, 9], and cell tracking [10, 11]. The ability to solubilize large amounts of gas into liquid PFCs has resulted in the development of oxygen delivery applications that may be useful for extending tissue viability during hypoxic events (such as cardiac bypass and hemorrhagic shock), enhancement of tumor radiation therapy, and liquid breathing [12–17]. Although some PFCs exhibit echogenicity due to a lower speed-of-sound and higher density than water [18–20], the contrast provided is much lower than that of MCAs. Some studies have shown that once bound to a surface, a liquid PFC-core agent can increase the acoustic reflectivity of the target, and that the reflectivity may be optimized by the choice of PFC [18, 21]. Additionally, liquid PFC-based agents are convenient for multimodal imaging beyond ultrasound either through endogenous PFC properties or through the inclusion of other agents. PFCs, particularly those with higher boiling points, carry a high number of fluorine atoms that can be used for $^{19}$F MR spectroscopy [22, 23]. Inclusion of paramagnetic nanoparticles, fluorescent nanoparticles, and/or radioisotopes enable these PFC emulsions to be extended to $^{1}$H MR T1-weighted imaging, SPECT-CT [4, 5, 8, 22, 23], and optical fluorescence imaging [10, 11]. Particular PFCs may also serve as radiopaque blood pool agents for CT due to the long intravascular half-life [1, 3, 9].

MCAs for diagnostic and therapeutic ultrasound have provided a promising platform for addressing a number of issues, including applications in echocardiography, microvascular perfusion imaging, thermal ablation enhancement, molecular imaging, drug and gene delivery, and thrombolysis [24–41]. PFCs have been favored for the gaseous core for more than a decade because of low solubility compared to other gases [42, 43]. MCAs are typically produced with diameters in the 1–5 μm range, which is a compromise between enabling free passage through capillary beds, and maximizing ultrasound imaging sensitivity. When excited by ultrasound energy, highly compressible microbubbles exhibit nonlinear behavior. This has led to microbubble-specific imaging modalities that enable contrast imaging with high sensitivity and low background signal from tissue [44–50]. However, sizes optimal for contrast enhancement limit passage to within the vascular space [38], and microbubble persistence *in vivo* is typically only on the order of minutes [43].

Preclinical studies have suggested that, in contrast to MCAs, PCCAs can be designed to have relative stability in circulation prior to ultrasound-induced vaporization. Once vaporized, they exhibit contrast enhancement similar to what MCAs provide [51–55]. Several reviews on MCAs [35, 56, 57], liquid PFC contrast agents [58], and methods of drug/gene delivery [59] have included discussions of PCCAs. In this review, a brief survey of the history of phase-change contrast agents and the multiple environmental, design, and ultrasound-based factors that influence droplet vaporization is presented. The many proposed applications at both the microscale and nanoscale are discussed with a summary of the *in vivo* studies performed to date that show promising results for future use in humans.

Issues involved with PCCA design as well as possibilities for future studies and applications are addressed.

## PHASE-CHANGE CONTRAST AGENTS: HISTORY AND INFLUENCING FACTORS

Although the general physics of droplet vaporization has been well-described in the literature, phase-transition as a result of ultrasound energy and the range of diagnostic and therapeutic possibilities for PCCAs have only begun to emerge in the past two decades. Phase-change colloids for ultrasonic imaging were first proposed by Quay in 1996 [60], resulting in development of the contrast agent EchoGen™ (Sonus Pharmaceuticals, Inc., Bothell, WA), although clinical trials were ultimately discontinued. EchoGen™ was fundamentally different in application than most PCCAs being developed currently in that stable emulsions of dodecafluoropentane (DDFP) were pre-conditioned to induce phase-transition into gas-filled contrast agents in the 2 – 5 μm diameter range prior to intravenous injection [61–63], rather than activation while in circulation. In 1998, Apfel proposed superheated droplets that, while circulating in vivo, could be activated with a degree of spatial specificity by ionizing radiation or ultrasound for enhanced diagnostic capability, drug delivery, and targeted vessel occlusion [64].

Perfluorocarbons and perfluorochemicals have been particularly attractive compounds in conjunction with PCCAs – not only due to the properties stated earlier, but also because many have boiling points near physiological temperatures, which allows for the design of droplets in or near a superheated state. Table **1** lists selected PFCs that have been used for inert liquid emulsions, MCAs, and PCCAs along with their physical properties, if available, gathered from several sources of literature [18, 20, 65]. DDFP, in particular, has been the most often-used compound because its boiling point of 29°C allows for the possibility of droplet generation at room temperature, and exposure to physiological temperatures results in a superheated droplet - although in practice, droplet size becomes a factor due to the effects of surface tension.

Surface tension plays a large role in both the threshold of vaporization for a droplet and the subsequent volumetric expansion. Beyond ambient pressure, a PFC droplet will experience an additional Laplace pressure as a result of surface tension effects over a defined radius [53, 66]:

$$\Delta P_{Laplace} = P_{Inside} - P_{Outside} = \frac{2\sigma}{r} \quad \text{(Equation \#1)}$$

where $P_{Inside}$ represents the pressure inside the droplet, $P_{Outside}$ represents the pressure outside the droplet, $\sigma$ represents surface tension, and $r$ represents radius. Although liquid PFCs have characteristically low interfacial surface tension with air, their hydrophobicity may lead to relatively high interfacial surface tension when dispersed in water [67, 68], and therefore the pressure exerted on the liquid core at the microscale and nanoscale may reach several atmospheres above ambient pressure. Through encapsulation in a lipid or polymer

shell, Kandadai and colleagues showed that the interfacial surface tension of DDFP droplets may be modified by the choice of emulsifier to provide more favorable properties for dispersion in aqueous media [68]. The relationship between the ambient pressure a compound experiences and the temperature required to induce phase-transition is approximated by the Antoine vapor-pressure equation, which is a derivation of the Clausius-Clapeyron relation. The Antoine vapor-pressure equation is defined as:

$$T = \frac{B}{A - \log_{10} P} - C \quad \text{(Equation \#2)}$$

where T is the ambient temperature, P is the ambient pressure exerted on the droplet, and A, B, and C are experimentally derived constants observed for a particular temperature range. The relation shows that as the pressure is raised on the droplet core, the energy (in the form of temperature and/or ultrasound) required to induce phase transition increases. Because the Laplace pressure is an inverse function of radius, this effect becomes more pronounced for droplets in the nanometer range. By ideal gas laws with surface tension included, once a PFC droplet is vaporized, the resulting bubble will theoretically expand approximately 3 – 6 times in diameter, depending on initial droplet size, ambient pressure, and the density of the PFC selected [66, 69]. Bubbles resulting from droplets at the nanoscale will experience a greater Laplace pressure than those resulting from droplets at the microscale, which will serve to compress the gas core to a greater extent. Therefore, expansion of droplets in the nanometer range is expected to be less than that of droplets in the micrometer range. As droplet size diminishes, the expansion factor will theoretically be dominated by the effect of surface tension/Laplace pressure, while the expansion factor for very large droplets (negligible Laplace pressure) becomes dominated by ambient pressure (Fig. **2**). A recent experimental study by Wong and colleagues aimed at elucidating the dynamics of bubble evolution suggested that, for micron-sized droplets of dodecafluoropentane, the phase transition may occur in stages following the initial vaporization event [70]. Once vaporized, the bubbles approached theoretical expansion predictions on a microsecond timescale, although this may differ with other PFC selections and encapsulations. Several studies have shown *in vitro* that bubbles may expand beyond ideal gas law predictions due to the influx of dissolved gases present in the surrounding media [66, 71, 72]. In theory, this additional expansion is likely to be more pronounced for larger bubbles than smaller bubbles, as the internal pressure of the gas core due to surface tension is less.

The exact mechanisms that cause a droplet to undergo a phase change as a result of ultrasonic energy – termed acoustic droplet vaporization (ADV) – are the subject of much discussion in the literature. Because the phase-transition boundary of a pure compound is governed by the relationship of temperature and vapor pressure, one hypothesis is that the phase-transition occurs due to acoustic heating of the droplet. Were this the sole mechanism, then increasing ultrasonic pulse duration should increase the degree of acoustic heating and trigger phase-transition of droplets. However, most studies have shown that increasing pulse duration at clinically relevant ultrasound frequencies results in no significant decrease in the vaporization pressure needed to achieve ADV, unless the duration is on the order of 1 millisecond or greater [73–76]. For these longer pulse lengths, a decrease in the ultrasound

pressure needed to induce vaporization has been observed. Although this may seem to be indicative of acoustically-induced heating, Lo and colleagues found that by using shorter periodic pulses unlikely to cause heating, but with an equivalent total 'on-time' as the longer pulses, a similar decrease in required ultrasound pressure resulted – indicating heating may not be the primary mechanism at work [74]. Other studies have provided convincing evidence that acoustic droplet vaporization may be initiated primarily by mechanical effects such as acoustic and hydrodynamic cavitation. Kripfgans and colleagues used high-speed optical microscopy to observe droplet deformations due to acoustic pressure, and showed that droplets with diameters in the micrometer range vaporized once a deformational threshold was reached, independent of original size [77]. More recent studies have shown vaporization can be induced independently of inertial acoustic cavitation, which has a number of implications for safety *in vivo* [75, 76].

Although the primary mechanism of ADV has not been completely revealed, a number of mathematical and physical models have been developed to simulate various properties of droplet vaporization. Ye and Bull have developed several models to describe the possible effects of post-vaporization expansion on wall stress to determine potential for damaging blood vessels [78, 79]. Other models have investigated the effect of surface tension on boiling point elevation, freezing point depression, volumetric expansion, and the oscillatory evolution of bubbles [69, 80]. Regardless of the primary mechanism, a large number of factors have been shown to influence the ultrasound pressure needed to induce vaporization of a droplet. These can be separated into three principle categories: environmental factors, droplet design, and ultrasound parameters (Table **2**). Many of the applications proposed for PCCAs stem from the numerous factors that influence their vaporization.

The stability of circulating PCCAs *in vivo* is not well-characterized to date, although a few studies have suggested that certain PCCAs show greater circulation times than their counterpart perfluorocarbon-filled MCAs. Rapoport and colleagues have published several *in vivo* studies using polymer-coated, drug-loaded DDFP nanodroplets suggesting that a significant amount of nanodroplets were still in circulation as much as 4–5 hours after intravenous injection in mice [52, 53, 81]. When subjecting these droplets to ultrasonic energy, a substantial reduction in tumor growth was achieved over controls. Recent studies from this group using higher boiling-point perfluorocarbons have suggested that the residence time may also be significantly influenced by the design of the encapsulating shell [54]. Zhang and colleagues recently published results showing that micron-sized droplets of DDFP were able to achieve an equivalent effect when activated 30 minutes after intravenous injection in a canine model compared to those activated immediately after injection, although they did not test timepoints beyond 30 minutes [55]. In general, it is likely that longevity in circulation will be a function of PFC boiling point, design of the encapsulating shell, and droplet size, although many preclinical studies are needed to characterize these effects *in vivo*.

## PCCA APPLICATIONS

Phase-change contrast agent applications can be roughly divided into two categories – those with droplets in the micrometer range and those with droplets in the nanometer range. While

droplets in both size categories have been proposed as drug delivery agents, droplets at the microscale, which are confined to vascular flow, hold unique possibilities for applications such as targeted vessel occlusion, ultrasound aberration correction, enhancing cavitation activity, and creation of internal markers for intraoperative guidance. Droplets at the nanoscale are primarily designed to take advantage of the well-studied enhanced permeability and retention (EPR) effect of solid tumors. As tumors grow and recruit new vasculature, the rapidly-formed vessels often exhibit a degree of 'loose' organization. Inter-endothelial gaps that normally prevent passage of large molecules into interstitial space are characteristically wider depending on tumor type, and can allow for extravasation of particles well in to the hundreds of nanometers in size.[86, 87] PCCAs that can take advantage of the EPR effect have been proposed for applications such as ultrasound-mediated drug delivery, diagnostic imaging, and enhanced thermal ablation. In both size ranges, droplets can be administered intra-arterially, intravenously, or through direct intra-tumoral injection and then vaporized [51, 88–90]. In a few cases, the applications proposed for nanoscale droplets are similar to those for microscale droplets – such as drug delivery to solid tumors and enhancing the effects of HIFU therapy. Future *in vivo* work will be needed to develop an understanding of the tradeoffs inherent in choosing to pursue these techniques with microscale vs. nanoscale droplets. The specific applications are discussed below.

## Microscale Applications

**Vascular Occlusion Agents—**Beginning with some of the earliest literature available on ADV, there has been significant interest in designing droplets in the micrometer size range for the purpose of vessel occlusion [51, 71]. Once vaporized, droplets near 5 μm in diameter will result in microbubbles that are on the order of 30 μm – sufficient to occlude microvasculature. By using focused ultrasound transducers, vaporization can be induced in the feeder arteries of kidneys (and by extension, tumors), resulting in the ability to occlude with a high degree of spatial specificity (Fig. **3**) [88, 90]. This type of occlusion may be especially beneficial in enhancing thermal therapy of tumors, such as in radio-frequency ablation. Often the blood supply of the tumor can act as a heat sink - dissipating the heat and reducing the efficacy of the treatment. By occluding nearby vasculature, thermal delivery may be more successful [88]. Reduced blood flow by occlusion may also be used to induce hypoxia in tumors, although future studies will be needed to determine whether the influence of PFC oxygen solubility reduces the degree of induced hypoxia in practice [51]. ADV-based occlusion appears to provide significant opportunity with regard to drug delivery. Residence time of drugs could be increased through reduced blood flow, allowing for enhanced diffusion into a targeted region. Drugs may be co-injected systemically or in the form of drug delivery vehicles such as liposomes, or alternately could be incorporated into the ADV occlusion agent through a dual-phase emulsion or multiple emulsions. Perhaps the most promising portrait for the potential of ADV-based occlusion was proffered by Fabiilli and colleagues [91]:

1. Through drug-incorporated emulsions, targeted occlusion can coincide with release of a chemical embolic agent – thus sustaining embolization.
2. The resulting ischemia may increase the residence time of a therapeutic agent locally, enhancing efficacy of therapeutic delivery.

3. Hypoxia as a result of prolonged ischemia may be useful for activation of bioreductive prodrugs – which potentially can be encapsulated in the emulsion process.

Although no *in vivo* validation is available to date, Fabiilli and colleagues have shown preliminary *in vitro* proof-of-concept of encapsulation of thrombin and chlorambucil in PCCA emulsions, followed by release with ultrasound-triggered vaporization [91, 92]. These studies also demonstrate the need for further optimization of formulation and drug loading as well as control over non-US-induced drug release and droplet size prior to preclinical studies. How these emulsion techniques perform compared to alternative platforms, such as microscale PFC droplets co-injected with drug-loaded liposomes or micelles, will also need to be characterized.

Ultimately, the success of ADV-based occlusion techniques depends on the dynamics involved in the transport and lodging of microbubbles generated from PCCAs. Due to a number of influencing factors, these bubbles may become lodged in the microvasculature near the site of vaporization, may slide along the vascular space, or may interact in a complex manner with vessel bifurcations downstream. It is also important that the occlusive bubbles not be so large as to damage or rupture the vessel wall. Several physical models have been developed by the University of Michigan group to simulate these dynamics [78–80, 93–96]. Although some experimental studies are available on non-ADV microbubble embolization [97, 98], further experimental results from ADV-generated microbubbles are needed to validate these models as they extend to pulsatile blood flow in the microvasculature.

**Aberration Correction—**Phase aberration of reconstructed ultrasound images is a result of cumulative error in estimating the speed-of-sound in the tissue the ultrasonic wave travels through. On the transmit side, this leads to the transducer not focusing as desired, and on the receive/reconstruction side results in poor, blurry images [51]. Aberration becomes especially prominent when imaging through dense tissue or bone – such as the skull, and worsens as ultrasound frequency increases. One proposed mechanism for aberration correction is to use disperse point targets in the form of echogenic gas bubbles at defined locations in the volume-of-interest. Using iterative methods, the ‘brightness’ of the point target can be used as a measure of aberration correction, and transducer timing can be adjusted to create optimal focusing and image reconstruction. Phase-change contrast agents present a unique opportunity for aberration correction in that low-concentration droplets can be vaporized with a degree of spatial specificity, lodge in a vessel, and create a stationary point beacon for iterative methods [51, 71, 99]. Preliminary results using acoustic droplet vaporization have been promising for focusing on transmit (Fig. **4**), but have not yet been extended to image reconstruction [99].

**Cavitation Nucleation Agents—**Bioeffects caused by ultrasound-induced cavitation *in vivo* range from cell sonoporation (increasing permeability of the cell wall) to cell lysis and tissue homogenization [100]. In addition, beyond certain pressure thresholds significant heating can occur [101]. These phenomena can be harnessed for both hyperthermic and non-thermal tumor treatments – such as cell lysis in combination with enhanced gene

transfection due to sonoporation. However, optimal tumor treatment would require precise spatial and temporal control of the cavitation events [82]. Cavitation nuclei are relatively sparse in blood and tissue, but it has been shown that microbubble contrast agents can act as cavitation nuclei and lower the energy needed to induce bioeffects [102–104]. As mentioned previously, microbubbles exhibit low circulation times *in vivo*, and so phase-change contrast agents may present a novel means of producing more stable cavitation nuclei with control of spatial and temporal activation for therapeutic applications. Early studies by Miller and colleagues have shown that hemolysis by lithotripter shock waves was more pronounced in the presence of PCCAs *in vitro* than for MCAs [82]. An *in vivo* study resulted in enhanced cell transfection of DNA plasmids and growth-rate reduction similar to that produced by MCAs and macroscopic air bubbles when all were injected intra-tumorally [105]. Lo and colleagues proposed that spatial control of droplet vaporization could be used to create predictable lesion formation and demonstrated the concept in tissue-mimicking phantoms [106]. A recent study by Zhang and colleagues showed that microscale droplets of DDFP significantly enhanced lesion formation *in vitro* as well as *in vivo* [55]. When droplets were introduced to tissue-mimicking phantoms, the exposure time needed to create similar lesions as controls was decreased by a factor of 2.5. When equal exposure times were used, the average lesion volume was 7-fold greater than phantoms without droplets. *In vivo* results proved even more promising, resulting in a 15-fold increase in volume for lesions formed in the canine liver at equal exposure time to controls without droplets.

**Internal Markers for Intraoperative Guidance—**One of the most recently-developed applications for PCCAs involves harnessing their sensitivity to heat and ultrasound pressure to create internal markers that may assist during therapeutic or surgical procedures. Huang and colleagues proposed a method where PCCAs designed to vaporized at a specific temperature are injected near the periphery of a tumor site and activated once the tissue reaches a lethal thermal dose - providing real-time feedback on intraoperative ablation margins [107]. They demonstrated this concept *in vitro* using micron-sized PLGA-encapsulated PCCAs. More recently, Couture and colleagues proposed ‘internal tattooing’, where PCCAs loaded with payloads of fluorescent markers are activated to release the fluorescent payload at the transducer focus [108]. This could be used to label areas of interest and delineate regions preoperatively with a high degree of spatial specificity that would then be visible intraoperatively through fluorescence imaging. They demonstrate proof-of-concept *in vivo* by ultrasonically activating PCCAs and labeling tissues at different locations in a chicken embryo.

## Nanoscale Applications

**Intra-tumoral Diagnostics and Therapeutic Delivery—**Phase-change contrast agents provide a novel means of addressing diagnostics and drug delivery of solid tumors. Kawabata and colleagues, who published some of the earliest studies of nanoscale PCCAs activated by ultrasound, showed successful vaporization of nanodroplets consisting of mixtures of liquid perfluorocarbons [84]. Through the EPR effect, droplets generated in the nanometer size range may diffuse out of the vascular space before undergoing phase-change triggered by ultrasound. By ideal gas laws with surface tension effects taken into account, droplets 200 nm or larger should result in gas microbubbles on the order of 1 μm [66, 69],

which would provide significant contrast enhancement of tumor interstitium. This would effectively extend microbubble-based imaging beyond the vascular space and create new opportunities for tumor detection and treatment. Rapoport and colleagues have proposed a multi-faceted imaging and treatment platform using nanoscale PCCAs with drug-loaded polymer shells in conjunction with drug-loaded micelles where ultrasound combined with droplet vaporization enhances local drug delivery (Fig. **5**) [109]. The resulting microbubbles (as well as larger secondary bubbles formed by coalescence) can be used as real-time delivery confirmation. Over a wide range of studies, her group has demonstrated the promise of PCCAs for delivery of paclitaxel and doxorubicin *in vitro* and *in vivo* for various cancer models using DDFP droplets encapsulated in a polymer shell [52, 53, 81, 89, 109–111]. The group has recently begun to explore the use of much higher boiling-point PFCs for increased stability, reversible bubble formation, and co-registration with $^{19}$F MRI, although they conclude that the temporary bubbles observed in the study may be due to gases dissolved in the PFC rather than actual vaporization of the PFC itself [54]. Matsuura and colleagues have provided promising preliminary evidence that incorporated nanoparticles such as quantum dots may act as additional cavitation nuclei within the core, and appear to decrease the ultrasound vaporization threshold significantly [85]. They suggest that PCCAs with incorporated nanoparticles may offer a means of spatially and temporally controlling nanoparticle deposition, and could produce a means to extend ADV-based agents to other therapeutic and imaging modalities.

**Thermal Ablation Therapy and Therapeutic Bioeffects—**PCCAs that have diffused into tumor interstitial space could also be used to aid in HIFU tumor ablation or to produce therapeutic bioeffects such as those that Miller and colleagues showed for microscale droplets. Once vaporized, the resulting bubbles can act as extravascular cavitation nuclei that enhance tissue heating and lesion formation from HIFU therapy. Although no published studies to date have explored the ability of nanoscale droplets to produce the bioeffects that Miller and colleagues observed at the microscale [82, 105], it is possible that nano-PCCAs may be similarly used to produce cell lysis, sonoporation, and enhanced gene transfer. Zhang and Porter have recently reported on the ability of PCCA nanodroplets to significantly enhance thermal delivery in the region of focus once vaporized in gel phantoms (Fig. **6**) [83]. They suggest that resulting interstitial bubbles *in vivo*, which would theoretically be in the low micrometer range, would have resonance frequencies similar to MCAs used in HIFU [112], and therefore would be uniquely suited for tumor ablation and lesion formation. Future studies are needed to characterize how interstitial bubbles produced by PCCAs interact with the HIFU beam, and the resulting effect on cavitation activities.

**Other Applications—**Nanoscale PCCAs were used by Mohan and Rapoport to aid in the study of intracellular delivery of doxorubicin, including factors that influence penetration into the cell nucleus [113]. Their results suggest that ultrasound in the presence of microbubbles, including those created by vaporized nanodroplets, transiently permeabilizes the cell nucleus and allows penetration of therapeutic drugs into the nucleus. Asami and colleagues have also proposed that nanoscale PCCAs could be used to characterize viscoelastic properties of tumors by analyzing the waveforms received post-vaporization [114].

## SELECTION OF PFCS

When designing phase-change contrast agents, the choice of which PFC comprises the core will create inherent trade-offs. As the energy needed to vaporize droplets of a certain size increases, the likelihood of inducing unwanted bioeffects for certain applications also increases. However, some applications may place a premium on high droplet stability over how easily the droplets can be vaporized. The optimal choice of PFC can largely be determined by considering:

1. The ideal size-regime of the droplets (nanoscale vs. microscale)
2. The ultrasound frequency used
3. Whether intended for diagnostic or therapeutic ultrasound machines
4. Whether ultrasound-induced bioeffects are acceptable

Droplets in the micrometer range require substantially less ultrasound pressure to induce vaporization than droplets in the nanometer range, presumably due to less Laplace pressure on the droplet core by interfacial surface tension. Additionally, the pressure required to vaporize decreases as the compound boiling point decreases. While increasing the ultrasound frequency has been shown to decrease the pressure needed to vaporize, higher frequencies will provide less penetration depth into tissues and will therefore limit the ability to successfully vaporize droplets in deep-tissue targets. Studies are needed to examine optimization of droplet vaporization as a function of frequency for deep-tissue targets *in vitro* and *in vivo*. For some applications, the ability to vaporize droplets from the lowest possible pressures would be ideal. In these cases, the droplets should be made from the PFC with the lowest possible boiling point that allows for stable circulation at physiological temperatures. For some therapeutic applications, the pressures used are already relatively high to create desired bioeffects, and droplets should remain stable until a desired ‘activation pulse’ is delivered. For these applications, PFCs with a higher boiling point may be more suitable.

Most studies have shown that for applications such as vascular occlusion and aberration correction, microscale dodecafluoropentane-based droplets appear to be sufficiently stable and are able to be vaporized *in vitro* at pressures within what diagnostic imaging machines typically provide [75, 76], although the pressures used to vaporize *in vivo* can be much higher [90]. DDFP and perfluorohexane (PFH) have been the most commonly-studied PFCs for use with nanoscale droplets. At these sizes, the optimal PFC choice is chiefly application-dependent. In a study with DDFP nanoemulsions for the purposes of enhancing thermal delivery to tumors and creating focal lesions, Zhang and Porter suggest that as the temperature rises in tissues, the nanodroplets just outside of the focal region may vaporize more easily and lead to unpredictable prefocal lesions [83]. A PFC with a higher boiling point, such as PFH, may prove better in this case, as it could still be vaporized and would lead to more predictable lesion formation. For co-imaging with $^{19}$F MR, a PFC with a higher number of Fluorine atoms per molecule may be desirable, although PFCs with more Fluorine atoms also have higher boiling points [54].

For some applications in both the nanometer and micrometer size regimes, it might be beneficial for the vaporization to occur at lower pressures than DDFP allows. Diagnostic image enhancement of tumors by extravasated nanodroplets requires that the droplets can be activated with little to no bioeffects, and by parameters within the range of a clinical imaging system. In addition, the degree of drug delivery or vascular occlusion from PCCAs is dictated partly by the efficiency of vaporization within the focal region, and so lower thresholds may lead to a greater number of vaporized droplets and increased drug delivery and/or flow reduction. While these issues may be improved by further optimizing ultrasound parameters such as frequency and pulse length, it is also possible to choose PFCs with lower boiling points than DDFP. A number of the previously mentioned *in vitro* studies have shown that DDFP droplets have remarkable stability at body temperature, even though the bulk boiling point of DDFP is much lower than body temperature. Presumably this is due to the increased internal pressure on the compound at the small sizes produced, which essentially increases the temperature required to vaporize the droplet. A study by Giesecke and Hynynen demonstrated that vaporizing micron-sized albumin-coated DDFP droplets by heat alone required temperatures as much as 40°C above the typical boiling point of DDFP as a bulk fluid [73], and the difference may increase as droplet size is reduced to the nanometer range. This increase in ‘effective boiling point’ leads to the possibility for lower boiling-point perfluorocarbons to be explored for PCCAs. This concept has been verified in two recent studies showing that decafluorobutane (DFB), which is normally a gas at room temperature, can be formed into nanoscale and microscale droplets that are stable *in vitro* at room and body temperature [66, 115]. These droplets can be vaporized at pressures significantly lower than similar droplets of DDFP and PFH, which is promising for applications requiring low acoustic pressures. Because DFB is a gas at room temperature, droplet generation techniques involved methods of condensing the gas at reduced temperatures and/or increased pressures. In the first study, droplets were produced by first condensing DFB gas at reduced temperatures and then encapsulating the resulting liquid DFB in lipid shells by membrane extrusion. The second study demonstrated a technique of ‘microbubble condensation’ to produce sub-micron droplets where lipid coated, micron-sized DFB microbubbles were generated via standard agitation techniques and then exposed to increased ambient pressure and decreased ambient temperature until condensation of the gas core occurred. Once condensed, the volumetric decrease resulted in sub-micron droplets that remained stable due to the increased internal pressure. Further studies are needed to determine overall *in vivo* stability of decafluorobutane droplets in both size ranges compared to previously explored PFCs, as well as to explore the possibility to stabilize droplets of lower boiling-point PFCs such as octafluoropropane.

One additional method of droplet design is to alter the amount of energy needed to vaporize a specific droplet by creating a mixture of PFCs with different boiling points. This technique was first proposed by Kawabata and colleagues, who demonstrated that mixing DDFP (b.p. 29°C) and 2H,3H-DDFP (b.p. 53°C) resulted in a droplet that required more energy to vaporized than if it contained only DDFP, but less than if it contained only 2H,3H-DDFP [84]. This technique could be useful in designing PCCAs for an optimal trade-off between stability in circulation and pressure required to induce vaporization.

## *IN VIVO* STUDIES

Although fewer articles are available for phase-change contrast agents compared to microbubbles and inert liquid PFC emulsions, a high proportion of the studies have shown promising *in vivo* results for a variety of animal models and anatomical targets – summarized in Table **3**. In general, researchers have shown that PCCAs are able to be vaporized *in vivo* to produce desired effects such as reduced blood perfusion and therapeutic drug delivery (Fig. **7**). In a few instances, droplet-induced bioeffects were observed. An early occlusion-based study by Kripfgans and colleagues using a rabbit model showed that filtering droplet emulsions to transcapillary sizes (99.99% < 6 μm in diameter) and lowering doses to approximately $2\times10^7$ droplets/kg eliminated instances of pulmonary hyperinflation [88]. They suggest that because the rabbit model may be more susceptible to this bioeffect [116], it may be possible to use much higher doses for greater embolization in humans. Another occlusion-based study in a canine model by Zhang and colleagues noted instances of cardiac arrhythmia and one instance of animal death when droplets (99.6% < 10 μm in diameter) were administered in doses on the order of $1\times10^8$ droplets/kg to $4\times10^8$ droplets/kg through an intracardiac method [90]. The effect seemed to stabilize once animals were placed on forced ventilation. They hypothesized that these effects were a result of droplets occluding a coronary arteriole, inducing ischemia. Although no cardiac arrhythmia was observed for intravenous administration, doses approaching $2\times10^9$ droplets/kg resulted in respiratory distress and changes in blood chemistry. A dose of $3\times10^9$ droplets/kg of droplets this size (a total perfluorocarbon dose of 0.2 g/kg) was determined to be fatal to the canines. In a recent study by Zhang and colleagues aimed at assessing microscale DDFP droplets for thermal ablation, a dose of $1.2\times10^8$ droplets/kg (99% < 8 μm in diameter) was administered intravenously in a canine model and no adverse bioeffects were reported [55]. All other studies noted no significant undesired bioeffects. Future studies are needed to optimize ultrasonic vaporization *in vivo* – especially with regard to reducing interference caused by respiratory motion in some animals [90].

## DISCUSSION

While the *in vivo* studies mentioned earlier have given ample evidence of the breadth that the PCCA platform may provide for future use in humans, more preclinical studies are needed to evaluate the potential for bioeffects as a result of PCCA administration. Characterizing the chemical effects of PFCs, possibility of vascular damage by very large bubbles, stability of agents in circulation, and ultrasound-induced effects from PCCAs combined with high pressures and/or pulse lengths will be vital in moving the platform toward clinical studies. For applications involving droplets extravasated via the EPR effect, the impact of diffusion gradients and uneven interstitial pressure within the tumor on the accumulation and delivery of drug payloads requires further investigation [89, 117]. Many studies have demonstrated that microscale droplets can be generated in sizes small enough to pass through human microvasculature without significant embolization until vaporization is induced [73, 76, 88]. To ensure safety while in circulation, further control of the droplet upper size limit has been demonstrated through filtering or microfluidic sorting [51, 73, 77, 106, 118, 119]. Current techniques of droplet generation typically result in polydisperse droplet sizes, and so developing new methods to generate monodisperse size distributions of

droplets may be useful in that droplets would respond more uniformly in the focal region of the transducer – both increasing the efficiency of the technique and reducing the chance of unwanted effects. Couture and colleagues demonstrated the use of microfluidics to create complex monodisperse PCCAs carrying fluorescent payloads [108]. Recent studies by Martz and colleagues [120] and Bardin and colleagues [121] have used microfluidics to generate monodisperse, microscale DDFP droplets that remain monodisperse for several weeks in storage. When vaporized by acoustic pressure, the droplets exhibit a highly uniform response – confirming the primary benefit of the production method. Techniques such as these may be advantageous for the future production and commercialization of PCCAs at the microscale.

Many possible applications of the PCCA platform await additional exploration:

1. Targeting ligands could be incorporated in the encapsulating shell to provide a means of PCCA-based molecular imaging similar to that of microbubbles and inert liquid PFC emulsions [33, 122–125], although no studies have been performed to date. The effect that incorporated ligands may have on *in vivo* aspects such as stability in circulation and clearance by the reticuloendothelial system will also need to be carefully addressed. Once vaporized, PCCAs may be manipulated to enhance targeting through ultrasound phenomena such as acoustic radiation force [126–128].

2. Studies have shown that lipid-coated microbubbles and liquid perfluorocarbon droplets can be internalized into neutrophils, macrophages, and tumor cells [129–132]. Kang and colleagues recently demonstrated preliminary studies of PCCA uptake into peritoneal macrophages followed by acoustic vaporization [133]. The internalization of targeted or non-targeted PCCAs into similar cells and subsequent vaporization could lead to new methods of tissue-specific treatments.

3. Several of the previously mentioned sources have either suggested or given preliminary demonstration of the possibility of co-imaging with CT and MR techniques, and through incorporation of nanoparticles this may be extended to additional modalities. Strohm and colleagues recently showed that incorporation of PbS nanoparticles into micron-sized droplets of DDFP allowed the droplets to be vaporized by near-infrared laser irradiation due to heat generated by the particles [134]. This may be harnessed in the future to develop new techniques in photoacoustic imaging

4. PCCAs could be co-injected with other platforms to create novel imaging and treatment techniques. Lo and colleagues showed that co-injection with MCAs significantly decreased the vaporization threshold for PCCAs by enhancing the acoustic field in the vicinity of the droplets [74]. Therefore, microbubbles, which could also be targeted for angiogenesis, might be useful in reducing the vaporization threshold for extravasated nanodroplets and improving drug delivery efficiency. A platform of drug-carrying liposomes/micelles and PCCAs could be developed such that the

vaporized droplets confirm therapeutic delivery and cavitation-based effects from the resulting bubbles enhance release of drugs. Finally, a co-injection of both nanoscale and microscale PCCAs could create a treatment where drugs are simultaneously released in the tumor interstitium by extravasated nanodroplets and in the vascular space by larger droplets that vaporize to form tissue-occluding microbubbles.

5. The nonlinear acoustic response from microbubbles excited in an ultrasound field has been harnessed to create contrast-specific techniques which can provide high contrast sensitivity while suppressing tissue background [46–50]. Two recent studies have demonstrated that the time-dependent spectral content of evolving bubbles resulting from vaporized PCCAs may have significantly different spectral information than MCAs [72, 135], which could lead to further contrast-specific imaging techniques.

## CONCLUSION

Phase-change contrast agents, which have properties of both the liquid emulsion and microbubble platforms, provide a unique set of tools to address *in vivo* and *in vitro* applications in novel ways. They can be generated over a wide range of useful sizes for diagnostic and therapeutic applications and can be manipulated in real-time, noninvasively, and with a non-ionizing imaging modality – ultrasound – that provides temporal and spatial specificity for droplet activation. In liquid form, they may be designed to exhibit smaller sizes and greater stability than MCAs, but once vaporized into microbubbles, result in marked contrast enhancement over surrounding tissue.

## Acknowledgments

The authors would like to thank Steven Feingold and Samantha Luois for perspicacious editing, and Dr. Terry Matsunaga for his expertise in perfluorocarbon nanoparticles. Paul Sheeran has been partly funded by a graduate fellowship from the National Science Foundation. The authors acknowledge support from the NIH from R21EB011704 (PI: Terry Matsunaga), as well as R01EB008733 and R01EB009066.

## References

1. Mattrey RF. The potential role of perfluorochemicals (PFCS) in diagnostic imaging. Artificial Cells, Blood Substitutes and Biotechnology. 1994; 22:295–313.
2. Krafft MP. Fluorocarbons and fluorinated amphiphiles in drug delivery and biomedical research. Advanced Drug Delivery Reviews. 2001; 47:209–228. [PubMed: 11311993]
3. Mattrey RF. Perfluorooctylbromide: A new contrast agent for CT, sonography, and MR imaging. Am J Roentgenol. 1989; 152:247–252. [PubMed: 2643258]
4. Lanza GM, Lorenz CH, Fischer SE, et al. Enhanced detection of thrombi with a novel fibrin-targeted magnetic resonance imaging agent. Acad Radiol. 1998; 5(Suppl 1):S173–S176. discussion S83-4. [PubMed: 9561074]
5. Flacke S, Fischer S, Scott MJ, et al. Novel MRI contrast agent for molecular imaging of fibrin: implications for detecting vulnerable plaques. Circulation. 2001; 104:1280–1285. [PubMed: 11551880]

6. Winter PM, Caruthers SD, Kassner A, et al. Molecular imaging of angiogenesis in nascent Vx-2 rabbit tumors using a novel αvβ3-targeted nanoparticle and 1.5 Tesla magnetic resonance imaging. Cancer Research. 2003; 63:5838–5843. [PubMed: 14522907]
7. Dayton PA, Zhao S, Bloch SH, et al. Application of ultrasound to selectively localize nanodroplets for targeted imaging and therapy. Mol Imaging. 2006; 5:160–174. [PubMed: 16954031]
8. Lanza G, Winter P, Caruthers S, et al. Theragnostics for tumor and plaque angiogenesis with perfluorocarbon nanoemulsions. Angiogenesis. 2010; 13:189–202. [PubMed: 20411320]
9. Behan M, O'Connell D, Mattrey R, Carney D. Perfluorooctylbromide as a contrast agent for CT and sonography: preliminary clinical results. Am. J. Roentgenol. 1993; 160:399–405. [PubMed: 8424361]
10. Partlow KC, Chen J, Brant JA, et al. 19F magnetic resonance imaging for stem/progenitor cell tracking with multiple unique perfluorocarbon nanobeacons. The FASEB Journal. 2007; 21:1647–1654. [PubMed: 17284484]
11. Srinivas M, Cruz LJ, Bonetto F, Heerschap A, Figdor CG, de Vries IJM. Customizable, multi-functional fluorocarbon nanoparticles for quantitative in vivo imaging using 19F MRI and optical imaging. Biomaterials. 2010; 31:7070–7077. [PubMed: 20566214]
12. Clark LC, Gollan F. Survival of mammals breathing organic liquids equilibrated with oxygen at atmospheric pressure. Science. 1966; 152:1755–1756. [PubMed: 5938414]
13. Biro GP, Blais P, Rosen AL. Perfluorocarbon blood substitutes. Critical Reviews in Oncology/Hematology. 1987; 6:311–374. [PubMed: 3549022]
14. Fuhrman BP, Paczan PR, DeFrancisis M. Perfluorocarbon-associated gas exchange. Crit Care Med. 1991; 19:712–722. [PubMed: 2026035]
15. Riess JG. Fluorocarbon-based in vivo oxygen transport and delivery systems. Vox Sang. 1991; 61:225–239. [PubMed: 1776239]
16. Holman WL, Spruell RD, Ferguson ER, et al. Tissue oxygenation with graded dissolved oxygen delivery during cardiopulmonary bypass. The Journal of Thoracic and Cardiovascular Surgery. 1995; 110:774–785. [PubMed: 7564446]
17. Koch CJ, Oprysko PR, Shuman AL, Jenkins WT, Brandt G, Evans SM. Radiosensitization of hypoxic tumor cells by dodecafluoropentane. Cancer Research. 2002; 62:3626–3629. [PubMed: 12097264]
18. Hall CS, Lanza GM, Rose JH, et al. Experimental determination of phase velocity of perfluorocarbons: Applications to targeted contrast agents. Ultrasonics, Ferroelectrics and Frequency Control, IEEE Transactions on. 2000; 47:75–84.
19. Pisani E, Tsapis N, Paris J, Nicolas V, Cattel L, Fattal E. Polymeric nano/microcapsules of liquid perfluorocarbons for ultrasonic imaging: Physical characterization. Langmuir. 2006; 22:4397–4402. [PubMed: 16618193]
20. Linstrom, PJ.; Mallard, WG., editors. NIST Chemistry WebBook, NIST Standard Reference Database Number 69. Gaithersburg: National Institute of Standards and Technology; 2011.
21. Marsh JN, Hall CS, Scott MJ, et al. Improvements in the ultrasonic contrast of targeted perfluorocarbon nanoparticles using an acoustic transmission line model. Ultrasonics, Ferroelectrics and Frequency Control, IEEE Transactions on. 2002; 49:29–38.
22. Lanza GM, Winter PM, Neubauer AM, et al. 1H/19F magnetic resonance molecular imaging with perfluorocarbon nanoparticles. Curr Top Dev Biol. 2005; 70:57–76. [PubMed: 16338337]
23. Caruthers SD, Neubauer AM, Hockett FD, et al. In vitro demonstration using 19F magnetic resonance to augment molecular imaging with paramagnetic perfluorocarbon nanoparticles at 1.5 Tesla. Investigative Radiology. 2006; 41:305–312. [PubMed: 16481914]
24. Porter TR, Xie F. Transient myocardial contrast after initial exposure to diagnostic ultrasound pressures with minute doses of intravenously injected microbubbles : Demonstration and potential mechanisms. Circulation. 1995; 92:2391–2395. [PubMed: 7586336]
25. Wei K, Jayaweera AR, Firoozan S, Linka A, Skyba DM, Kaul S. Quantification of myocardial blood flow with ultrasound-induced destruction of microbubbles administered as a constant venous infusion. Circulation. 1998; 97:473–483. [PubMed: 9490243]

26. Chomas JE, Pollard RE, Sadlowski AR, Griffey SM, Wisner ER, Ferrara KW. Contrast-enhanced US of microcirculation of superficially implanted tumors in rats. Radiology. 2003; 229:439–446. [PubMed: 14526091]
27. Miller DL, Thomas RM. Ultrasound contrast agents nucleate inertial cavitation in vitro. Ultrasound in Medicine & Biology. 1995; 21:1059–1065. [PubMed: 8553500]
28. Klibanov AL, Hughes MS, Marsh JN, et al. Targeting of ultrasound contrast material. An in vitro feasibility study. Acta Radiol Suppl. 1997; 412:113–120. [PubMed: 9240089]
29. Price RJ, Skyba DM, Kaul S, Skalak TC. Delivery of colloidal particles and red blood cells to tissue through microvessel ruptures created by targeted microbubble destruction with ultrasound. Circulation. 1998; 98:1264–1267. [PubMed: 9751673]
30. Lawrie A, Brisken AF, Francis SE, Cumberland DC, Crossman DC, Newman CM. Microbubble-enhanced ultrasound for vascular gene delivery. Gene Ther. 2000; 7:2023–2027. [PubMed: 11175314]
31. Tachibana K, Tachibana S. Albumin microbubble echo-contrast material as an enhancer for ultrasound accelerated thrombolysis. Circulation. 1995; 92:1148–1150. [PubMed: 7648659]
32. Klibanov AL. Microbubble contrast agents: targeted ultrasound imaging and ultrasound-assisted drug-delivery applications. Invest Radiol. 2006; 41:354–362. [PubMed: 16481920]
33. Ferrara K, Pollard R, Borden M. Ultrasound microbubble contrast agents: fundamentals and application to gene and drug delivery. Annual review of biomedical engineering. 2007; 9:415–447.
34. Luo W, Zhou X, Ren X, Zheng M, Zhang J, He G. Enhancing effects of SonoVue, a microbubble sonographic contrast agent, on high-intensity focused ultrasound ablation in rabbit livers in vivo. J Ultrasound Med. 2007; 26:469–476. [PubMed: 17384044]
35. Hernot S, Klibanov AL. Microbubbles in ultrasound-triggered drug and gene delivery. Advanced Drug Delivery Reviews. 2008; 60:1153–1166. [PubMed: 18486268]
36. Lindner JR. Contrast ultrasound molecular imaging of inflammation in cardiovascular disease. Cardiovasc Res. 2009; 84:182–189. [PubMed: 19783842]
37. Sboros V, Tang MX. The assessment of microvascular flow and tissue perfusion using ultrasound imaging. Proc Inst Mech Eng H. 2010; 224:273–290. [PubMed: 20349819]
38. Gessner R, Dayton PA. Advances in molecular imaging with ultrasound. Mol Imaging. 2010; 9:117–127. [PubMed: 20487678]
39. Staub D, Schinkel AF, Coll B, et al. Contrast-enhanced ultrasound imaging of the vasa vasorum: from early atherosclerosis to the identification of unstable plaques. JACC Cardiovasc Imaging. 2010; 3:761–771. [PubMed: 20633855]
40. Hitchcock KE, Holland CK. Ultrasound-assisted thrombolysis for stroke therapy: Better thrombus break-up with bubbles. Stroke. 2010; 41:S50–S53. [PubMed: 20876505]
41. Stride EP, Coussios CC. Cavitation and contrast: the use of bubbles in ultrasound imaging and therapy. Proceedings of the Institution of Mechanical Engineers, Part H: Journal of Engineering in Medicine. 2010; 224:171–191.
42. Porter, TR., inventor. The Board of Regents of the University of Nebraska, assignee. Ultrasound contrast agents and methods for their manufacture and use. United States patent US. 5,567,415. 1996 Oct.
43. Mullin L, Gessner R, Kwan J, Kaya M, Borden MA, Dayton PA. Effect of anesthesia carrier gas on in vivo circulation times of ultrasound microbubble contrast agents in rats. Contrast Media Mol Imaging. 2011; 6:126–131. [PubMed: 21246710]
44. Goldberg, BB.; Raichlen, JS.; Forsberg, F., editors. Ultrasound contrast agents: Basic principles and clinical applications. London: Martin Dunitz Ltd; 2001.
45. Pomper, MG.; Gelovani, JG., editors. Molecular imaging in oncology. New York: Informa Healthcare USA, Inc.; 2008.
46. Simpson DH, Chien Ting C, Burns PN. Pulse inversion Doppler: a new method for detecting nonlinear echoes from microbubble contrast agents. Ultrasonics, Ferroelectrics and Frequency Control, IEEE Transactions on. 1999; 46:372–382.
47. Forsberg F, Shi WT, Goldberg BB. Subharmonic imaging of contrast agents. Ultrasonics. 2000; 38:93–98. [PubMed: 10829636]

48. Shi WT, Forsberg F. Ultrasonic characterization of the nonlinear properties of contrast microbubbles. Ultrasound in Medicine & Biology. 2000; 26:93–104. [PubMed: 10687797]
49. Bouakaz A, Frigstad S, Ten Cate FJ, de Jong N. Super harmonic imaging: a new imaging technique for improved contrast detection. Ultrasound in Medicine & Biology. 2002; 28:59–68. [PubMed: 11879953]
50. Kruse DE, Ferrara KW. A new imaging strategy using wideband transient response of ultrasound contrast agents. IEEE Trans Ultrason Ferroelectr Freq Control. 2005; 52:1320–1329. [PubMed: 16245601]
51. Kripfgans OD, Fowlkes JB, Woydt M, Eldevik OP, Carson PL. In vivo droplet vaporization for occlusion therapy and phase aberration correction. Ultrasonics, Ferroelectrics and Frequency Control, IEEE Transactions on. 2002; 49:726–738.
52. Rapoport N, Gao Z, Kennedy A. Multifunctional nanoparticles for combining ultrasonic tumor imaging and targeted chemotherapy. J Natl Cancer Inst. 2007; 99:1095–1106. [PubMed: 17623798]
53. Rapoport NY, Kennedy AM, Shea JE, Scaife CL, Nam KH. Controlled and targeted tumor chemotherapy by ultrasound-activated nanoemulsions/microbubbles. J Control Release. 2009; 138:268–276. [PubMed: 19477208]
54. Rapoport N, Nam K-H, Gupta R, et al. Ultrasound-mediated tumor imaging and nanotherapy using drug loaded, block copolymer stabilized perfluorocarbon nanoemulsions. Journal of Controlled Release. 2011; 153:4–15. [PubMed: 21277919]
55. Zhang M, Fabiilli ML, Haworth KJ, et al. Acoustic droplet vaporization for enhancement of thermal ablation by high intensity focused ultrasound. Acad Radiol. 2011
56. Brujan E-A. Cardiovascular cavitation. Medical Engineering & Physics. 2009; 31:742–751. [PubMed: 19359210]
57. Wilson SR, Burns PN. Microbubble-enhanced US in body imaging: what role? Radiology. 2010; 257:24–39. [PubMed: 20851938]
58. Diaz-Lopez R, Tsapis N, Fattal E. Liquid perfluorocarbons as contrast agents for ultrasonography and (19)F-MRI. Pharm Res. 2010; 27:1–16. [PubMed: 19902338]
59. Husseini GA, Pitt WG. Micelles and nanoparticles for ultrasonic drug and gene delivery. Advanced Drug Delivery Reviews. 2008; 60:1137–1152. [PubMed: 18486269]
60. Quay, SC., inventor. Sonus Pharmaceuticals, Inc., assignee. Phase shift colloids as ultrasound contrast agents. United States patent US. 5,558,853. 1996 May.
61. Correas JM, Quay SD. EchoGen emulsion: a new ultrasound contrast agent based on phase shift colloids. Clin Radiol. 1996; 51(Suppl 1):11–14. [PubMed: 8605764]
62. Grayburn P. Perflenapent emulsion (echogen®): A new long-acting phase-shift agent for contrast echocardiography. Clinical Cardiology. 1997; 20:12–18.
63. Quay, SC.; Kessler, DR.; Roy, RA.; Worah, D., inventors. Sonus Pharmaceuticals, Inc., assignee. Nucleation and activation of a liquid-in-liquid emulsion for use in ultrasound imaging. United States patent US. 5,897,851. 1999 Apr.
64. Apfel, RE., inventor. Apfel Enterprises, Inc., assignee. Activatable infusable dispersions containing drops of a superheated liquid for methods of therapy and diagnosis. United States patent US. 5,840,276. 1998 Nov.
65. Freire MG, Carvalho PJ, Queimada AJ, Marrucho IM, Coutinho JAP. Surface tension of liquid fluorocompounds. Journal of Chemical & Engineering Data. 2006; 51:1820–1824.
66. Sheeran PS, Wong VP, Luois S, et al. Decafluorobutane as a phase-change contrast agent for low-energy extravascular ultrasonic imaging. Ultrasound in Medicine & Biology. 2011; 37:1518–1530. [PubMed: 21775049]
67. Clasohm LY, Vakarelski IU, Dagastine RR, Chan DYC, Stevens GW, Grieser F. Anomalous pH dependent stability behavior of surfactant-free nonpolar oil drops in aqueous electrolyte solutions. Langmuir. 2007; 23:9335–9340. [PubMed: 17665938]
68. Kandadai MA, Mohan P, Lin G, Butterfield A, Skliar M, Magda JJ. Comparison of surfactants used to prepare aqueous perfluoropentane emulsions for pharmaceutical applications. Langmuir. 2010; 26:4655–4660. [PubMed: 20218695]

69. Evans DR, Parsons DF, Craig VSJ. Physical properties of phase-change emulsions. Langmuir. 2006; 22:9538–9545. [PubMed: 17073477]
70. Wong ZZ, Kripfgans OD, Qamar A, Fowlkes JB, Bull JL. Bubble evolution in acoustic droplet vaporization at physiological temperature via ultra-high speed imaging. Soft Matter. 2011; 7:4009–4016.
71. Kripfgans OD, Fowlkes JB, Miller DL, Eldevik OP, Carson PL. Acoustic droplet vaporization for therapeutic and diagnostic applications. Ultrasound in Medicine & Biology. 2000; 26:1177–1189. [PubMed: 11053753]
72. Reznik N, Williams R, Burns PN. Investigation of vaporized submicron perfluorocarbon droplets as an ultrasound contrast agent. Ultrasound in Medicine & Biology. 2011; 37:1271–1279. [PubMed: 21723449]
73. Giesecke T, Hynynen K. Ultrasound-mediated cavitation thresholds of liquid perfluorocarbon droplets in vitro. Ultrasound Med Biol. 2003; 29:1359–1365. [PubMed: 14553814]
74. Lo AH, Kripfgans OD, Carson PL, Rothman ED, Fowlkes JB. Acoustic droplet vaporization threshold: effects of pulse duration and contrast agent. Ultrasonics, Ferroelectrics and Frequency Control, IEEE Transactions on. 2007; 54:933–946.
75. Fabiilli ML, Haworth KJ, Fakhri NH, Kripfgans OD, Carson PL, Fowlkes JB. The role of inertial cavitation in acoustic droplet vaporization. Ultrasonics, Ferroelectrics and Frequency Control, IEEE Transactions on. 2009; 56:1006–1017.
76. Schad KC, Hynynen K. In vitro characterization of perfluorocarbon droplets for focused ultrasound therapy. Phys Med Biol. 2010; 55:4933–4947. [PubMed: 20693614]
77. Kripfgans OD, Fabiilli ML, Carson PL, Fowlkes JB. On the acoustic vaporization of micrometer-sized droplets. The Journal of the Acoustical Society of America. 2004; 116:272–281. [PubMed: 15295987]
78. Ye T, Bull JL. Direct Numerical Simulations of Micro-Bubble Expansion in Gas Embolotherapy. Journal of Biomechanical Engineering. 2004; 126:745–759. [PubMed: 15796333]
79. Ye T, Bull JL. Microbubble Expansion in a Flexible Tube. Journal of Biomechanical Engineering. 2006; 128:554–563. [PubMed: 16813446]
80. Qamar A, Wong ZZ, Fowlkes JB, Bull JL. Dynamics of acoustic droplet vaporization in gas embolotherapy. Appl Phys Lett. 2010; 96:143702. [PubMed: 20448802]
81. Gao Z, Kennedy AM, Christensen DA, Rapoport NY. Drug-loaded nano/microbubbles for combining ultrasonography and targeted chemotherapy. Ultrasonics. 2008; 48:260–270. [PubMed: 18096196]
82. Miller DL, Kripfgans OD, Fowlkes JB, Carson PL. Cavitation nucleation agents for nonthermal ultrasound therapy. The Journal of the Acoustical Society of America. 2000; 107:3480–3486. [PubMed: 10875392]
83. Zhang P, Porter T. An in vitro study of a phase-shift nanoemulsion: a potential nucleation agent for bubble-enhanced HIFU tumor ablation. Ultrasound Med Biol. 2010; 36:1856–1866. [PubMed: 20888685]
84. Kawabata, K-i; Sugita, N.; Yoshikawa, H.; Azuma, T.; Umemura, S-i. Nanoparticles with multiple perfluorocarbons for controllable ultrasonically induced phase shifting. Jpn J Appl Phys. 2005; 44:5.
85. Matsuura N, Williams R, Gorelikov I, et al. Nanoparticle-loaded perfluorocarbon droplets for imaging and therapy. Ultrasonics Symposium (IUS), 2009 IEEE International. 2009:5–8.
86. Hobbs SK, Monsky WL, Yuan F, et al. Regulation of transport pathways in tumor vessels: Role of tumor type and microenvironment. Proceedings of the National Academy of Sciences. 1998; 95:4607–4612.
87. Campbell RB. Tumor physiology and delivery of nanopharmaceuticals. Anticancer Agents Med Chem. 2006; 6:503–512. [PubMed: 17100555]
88. Kripfgans OD, Orifici CM, Carson PL, Ives KA, Eldevik OP, Fowlkes JB. Acoustic droplet vaporization for temporal and spatial control of tissue occlusion: a kidney study. Ultrasonics, Ferroelectrics and Frequency Control, IEEE Transactions on. 2005; 52:1101–1110.
89. Rapoport N, Kennedy AM, Shea JE, Scaife CL, Nam KH. Ultrasonic nanotherapy of pancreatic cancer: lessons from ultrasound imaging. Mol Pharm. 2010; 7:22–31. [PubMed: 19899813]

90. Zhang M, Fabiilli ML, Haworth KJ, et al. initial investigation of acoustic droplet vaporization for occlusion in canine kidney. Ultrasound in Medicine & Biology. 2010; 36:1691–1703. [PubMed: 20800939]
91. Fabiilli M, Lee J, Kripfgans O, Carson P, Fowlkes J. Delivery of water-soluble drugs using acoustically triggered perfluorocarbon double emulsions. Pharmaceutical Research. 2010; 27:2753–2765. [PubMed: 20872050]
92. Fabiilli ML, Haworth KJ, Sebastian IE, Kripfgans OD, Carson PL, Fowlkes JB. Delivery of Chlorambucil using an acoustically-triggered perfluoropentane emulsion. Ultrasound in Medicine & Biology. 2010; 36:1364–1375. [PubMed: 20691925]
93. Calderon AJ, Fowlkes JB, Bull JL. Bubble splitting in bifurcating tubes: a model study of cardiovascular gas emboli transport. Journal of Applied Physiology. 2005; 99:479–487. [PubMed: 15790688]
94. Eshpuniyani B, Fowlkes JB, Bull JL. A bench top experimental model of bubble transport in multiple arteriole bifurcations. International Journal of Heat and Fluid Flow. 2005; 26:865–872.
95. Eshpuniyani B, Fowlkes JB, Bull JL. A boundary element model of microbubble sticking and sliding in the microcirculation. International Journal of Heat and Mass Transfer. 2008; 51:5700–5711. [PubMed: 19885367]
96. Calderon AJ, Eshpuniyani B, Fowlkes JB, Bull JL. A boundary element model of the transport of a semi-infinite bubble through a microvessel bifurcation. Physics of Fluids. 2010; 22:11.
97. Kort A, Kronzon I. Microbubble formation: In vitro and in vivo observation. Journal of Clinical Ultrasound. 1982; 10:117–120. [PubMed: 6804513]
98. Suzuki A, Armstead SC, Eckmann DM. Surfactant reduction in embolism bubble adhesion and endothelial damage. Anesthesiology. 2004; 101:97–103. [PubMed: 15220777]
99. Haworth KJ, Fowlkes JB, Carson PL, Kripfgans OD. Towards aberration correction of transcranial ultrasound using acoustic droplet vaporization. Ultrasound in Medicine & Biology. 2008; 34:435–445. [PubMed: 17935872]
100. Miller MW, Miller DL, Brayman AA. A review of in vitro bioeffects of inertial ultrasonic cavitation from a mechanistic perspective. Ultrasound in Medicine & Biology. 1996; 22:1131–1154. [PubMed: 9123638]
101. Holt RG, Roy RA. Measurements of bubble-enhanced heating from focused, mhz-frequency ultrasound in a tissue-mimicking material. Ultrasound in Medicine & Biology. 2001; 27:1399–1412. [PubMed: 11731053]
102. Miller DL, Thomas RM. Contrast-agent gas bodies enhance hemolysis induced by lithotripter shock waves and high-intensity focused ultrasound in whole blood. Ultrasound in Medicine & Biology. 1996; 22:1089–1095. [PubMed: 9004433]
103. Poliachik SL, Chandler WL, Mourad PD, et al. Effect of high-intensity focused ultrasound on whole blood with and without microbubble contrast agent. Ultrasound in Medicine & Biology. 1999; 25:991–998. [PubMed: 10461729]
104. Tran BC, Jongbum S, Hall TL, Fowlkes JB, Cain CA. Microbubble-enhanced cavitation for noninvasive ultrasound surgery. Ultrasonics, Ferroelectrics and Frequency Control, IEEE Transactions on. 2003; 50:1296–1304.
105. Miller DL, Song J. Lithotripter shock waves with cavitation nucleation agents produce tumor growth reduction and gene transfer in vivo. Ultrasound in Medicine & Biology. 2002; 28:1343–1348. [PubMed: 12467861]
106. Lo AH, Kripfgans OD, Carson PL, Fowlkes JB. Spatial control of gas bubbles and their effects on acoustic fields. Ultrasound in Medicine & Biology. 2006; 32:95–106. [PubMed: 16364801]
107. Huang J, Xu JS, Xu RX. Heat-sensitive microbubbles for intraoperative assessment of cancer ablation margins. Biomaterials. 2010; 31:1278–1286. [PubMed: 19942283]
108. Couture O, Faivre M, Pannacci N, et al. Ultrasound internal tattooing. Medical Physics. 2011; 38:1116–1123. [PubMed: 21452748]
109. Rapoport NY, Nam KH, Gao Z, Kennedy A. Application of ultrasound for targeted nanotherapy of malignant tumors. Acoust Phys. 2009; 55:594–601. [PubMed: 20160872]

110. Rapoport NY, Efros AL, Christensen DA, Kennedy AM, Nam KH. microbubble generation in phase-shift nanoemulsions used as anticancer drug carriers. Bubble Sci Eng Technol. 2009; 1:31–39. [PubMed: 20046899]
111. Rapoport N, Christensen DA, Kennedy AM, Nam K-H. Cavitation properties of block copolymer stabilized phase-shift nanoemulsions used as drug carriers. Ultrasound in Medicine & Biology. 2010; 36:419–429. [PubMed: 20133040]
112. Sassaroli E, Hynynen K. Resonance frequency of microbubbles in small blood vessels: a numerical study. Physics in Medicine and Biology. 2005; 50:5293. [PubMed: 16264254]
113. Mohan P, Rapoport N. Doxorubicin as a molecular nanotheranostic agent: Effect of Doxorubicin encapsulation in micelles or nanoemulsions on the ultrasound-mediated intracellular delivery and nuclear trafficking. Molecular Pharmaceutics. 2010; 7:1959–1973. [PubMed: 20957997]
114. Asami R, Ikeda T, Azuma T, Umemura S-i, Kawabata K-i. Acoustic signal characterization of phase change nanodroplets in tissue-mimicking phantom gels. Jpn J Appl Phys. 2010:49.
115. Sheeran PS, Luois S, Dayton PA, Matsunaga TO. Formulation and acoustic studies of a new phase-shift agent for diagnostic and therapeutic ultrasound. Langmuir. 2011; 27:10412–10420. [PubMed: 21744860]
116. Riess JG. The design and development of improved fluorocarbon-based products for use in medicine and biology. Artificial Cells Blood Substitutes and Immobilization Biotechnology. 1994; 22:215–234.
117. Ferretti S, Allegrini PR, Becquet MM, McSheehy PM. Tumor interstitial fluid pressure as an early-response marker for anticancer therapeutics. Neoplasia. 2009; 11:874–881. [PubMed: 19724681]
118. Huh D, Bahng JH, Ling Y, et al. Gravity-Driven Microfluidic Particle Sorting Device with Hydrodynamic Separation Amplification. Analytical Chemistry. 2007; 79:1369–1376. [PubMed: 17297936]
119. Nieuwstadt HA, Seda R, Li DS, Fowlkes JB, Bull JL. Microfluidic particle sorting utilizing inertial lift force. Biomedical Microdevices. 2010; 13:97–105. [PubMed: 20865451]
120. Martz TD, Sheeran PS, Bardin D, Lee AP, Dayton PA. Precision manufacture of phase-change perfluorocarbon droplets using microfluidics. Ultrasound Med Biol. 2011; 37:1952–1957. [PubMed: 21963036]
121. Bardin D, Martz TD, Sheeran PS, Shih R, Dayton PA, Lee AP. High-speed, clinical-scale microfluidic generation of stable phase-change droplets for gas embolotherapy. Lab Chip. 2011; 11:3990–3998. [PubMed: 22011845]
122. Lanza GM, Wickline SA. Targeted ultrasonic contrast agents for molecular imaging and therapy. Progress in Cardiovascular Diseases. 2001; 44:13–31. [PubMed: 11533924]
123. Hamilton AJ, Huang S-L, Warnick D, et al. Intravascular ultrasound molecular imaging of atheroma components in vivo. Journal of the American College of Cardiology. 2004; 43:453–460. [PubMed: 15013130]
124. Klibanov AL. Ligand-carrying gas-filled microbubbles:Ultrasound contrast agents for targeted molecular imaging. Bioconjugate Chemistry. 2004; 16:9–17. [PubMed: 15656569]
125. Lindner JR. Molecular imaging with contrast ultrasound and targeted microbubbles. Journal of Nuclear Cardiology. 2004; 11:215–221. [PubMed: 15052252]
126. Dayton P, Klibanov A, Brandenburger G, Ferrara K. Acoustic radiation force in vivo: a mechanism to assist targeting of microbubbles. Ultrasound in Medicine & Biology. 1999; 25:1195–1201. [PubMed: 10576262]
127. Rychak JJ, Klibanov AL, Hossack JA. Acoustic radiation force enhances targeted delivery of ultrasound contrast microbubbles: in vitro verification. Ultrasonics, Ferroelectrics and Frequency Control, IEEE Transactions on. 2005; 52:421–433.
128. Lum AFH, Borden MA, Dayton PA, Kruse DE, Simon SI, Ferrara KW. Ultrasound radiation force enables targeted deposition of model drug carriers loaded on microbubbles. Journal of Controlled Release. 2006; 111:128–134. [PubMed: 16380187]
129. Barbarese E, Ho S-Y, D'Arrigo JS, Simon RH. Internalization of microbubbles by tumor cells in vivo and in vitro. Journal of Neuro-Oncology. 1995; 26:25–34. [PubMed: 8583242]

130. Dayton PA, Chomas JE, Lum AF, et al. Optical and acoustical dynamics of microbubble contrast agents inside neutrophils. Biophys J. 2001; 80:1547–1556. [PubMed: 11222315]

131. Yanagisawa K, Moriyasu F, Miyahara T, Yuki M, Iijima H. Phagocytosis of ultrasound contrast agent microbubbles by Kupffer cells. Ultrasound in Medicine & Biology. 2007; 33:318–325. [PubMed: 17207907]

132. Kornmann L, Curfs D, Hermeling E, et al. Perfluorohexane-loaded macrophages as a novel ultrasound contrast agent: A feasibility study. Molecular Imaging and Biology. 2008; 10:264–270. [PubMed: 18536974]

133. Kang S-T, Yeh C-K. Intracellular acoustic droplet vaporization in a single peritoneal macrophage for drug delivery applications. Langmuir. 2011; 27:13183–13188. [PubMed: 21936541]

134. Strohm E, Rui M, Gorelikov I, Matsuura N, Kolios M. Vaporization of perfluorocarbon droplets using optical irradiation. Biomed Opt Express. 2011; 2:1432–1442. [PubMed: 21698007]

135. Kawabata K, Asami R, Azuma T, Umemura S. Acoustic response of microbubbles derived from phase-change nanodroplet. Jpn J Appl Phys. 2010; 49:9.

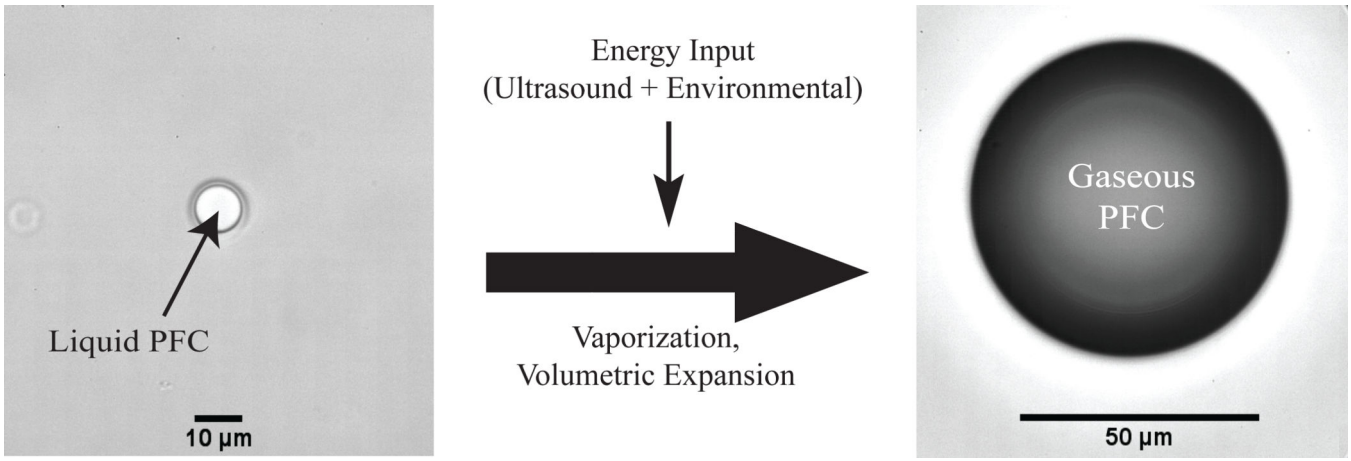


**Fig. (1).**

Vaporization of PFC droplets as a result of exposure to ultrasonic pulses. Shown here, a droplet of dodecafluoropentane encapsulated in a lipid shell is stable *in vitro* at 37°C, but vaporizes upon exposure to a 5 MHz ultrasonic pulse. The phase-transition results in a bubble approximately 5–6 times larger (unpublished data).

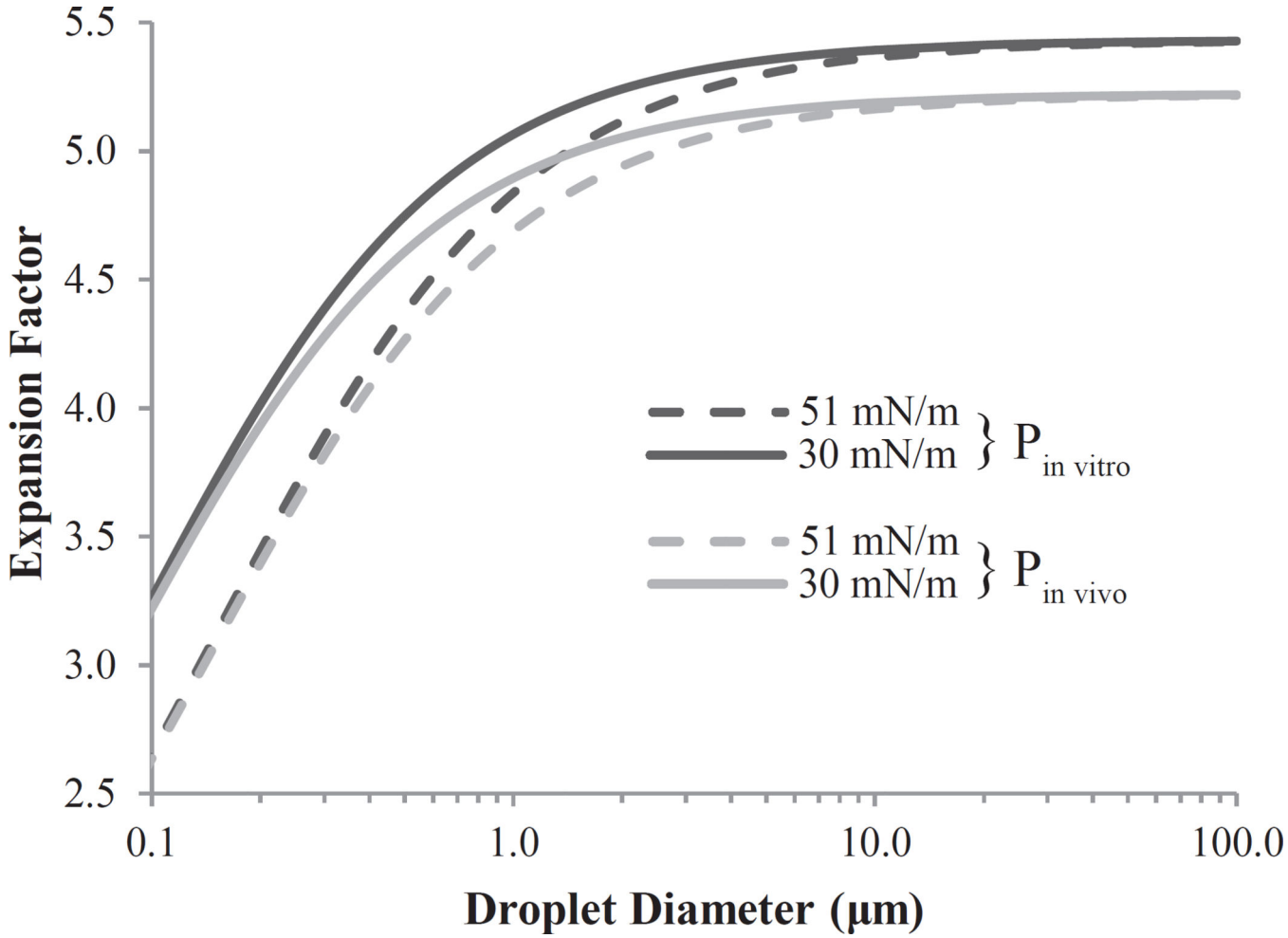


**Fig. (2).**

Effect of droplet size on expansion factor according to ideal gas laws with Laplace pressure included for a selected PFC. Calculations are presented for two variations of both ambient pressure ($P_{in\ vitro} \approx 101$ kPa; $P_{in\ vivo} \approx 114$ kPa) and surface tension ($\sigma_1 = 30$ mN/m; $\sigma_2 = 51$ mN/m). Expansion of droplets on the order of 10 μm is primarily dependent on ambient pressure, while expansion of droplets 500 nm or less is primarily dependent on surface tension. Reprinted from *Ultrasound in Medicine & Biology*, Vol. 37, Sheeran PS, Wong VP, Luois S, *et al.*, "Decafluorobutane as a phase-change contrast agent for low-energy extravascular ultrasonic imaging", 1518-30 (2011), with permission from Elsevier.

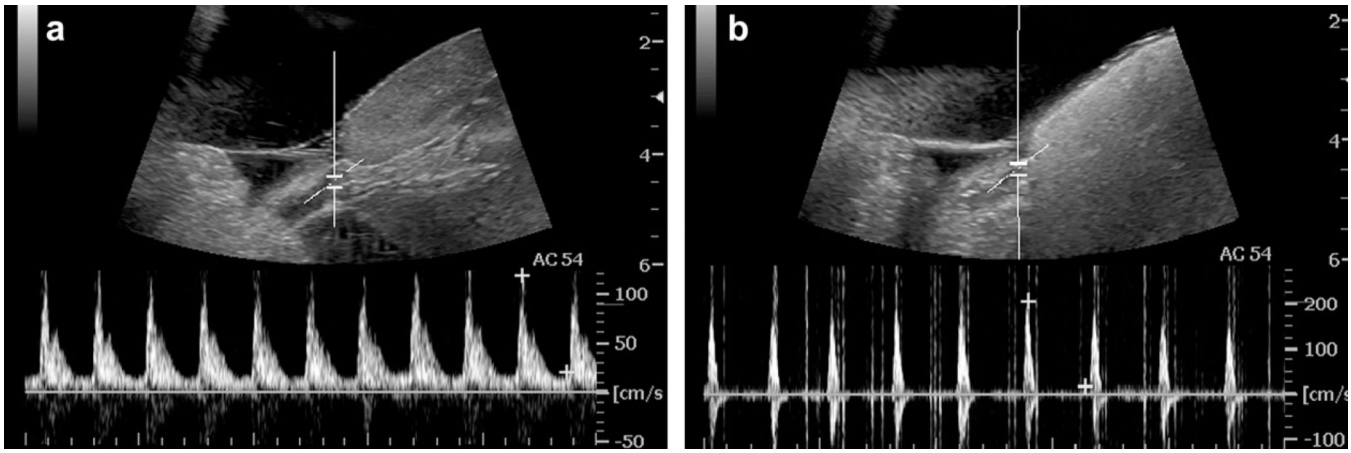


**Fig. (3).**

PCCA tissue occlusion demonstrated in a canine kidney with droplets injected intravenously. Pulse-wave Doppler spectrum taken at the targeted spot in the renal artery before (a) and immediately after ADV (b), where blood flow reversal and narrowing of the waveform along with significant shadowing in the kidney is observed possibly because of substantial vascular occlusion. Reprinted from *Ultrasound in Medicine & Biology*, Vol. 52, Zhang M, Fabiilli ML, Haworth KJ, *et al.*, "Initial investigation of acoustic droplet vaporization for occlusion in canine kidney", 1691–703 (2010), with permission from Elsevier.

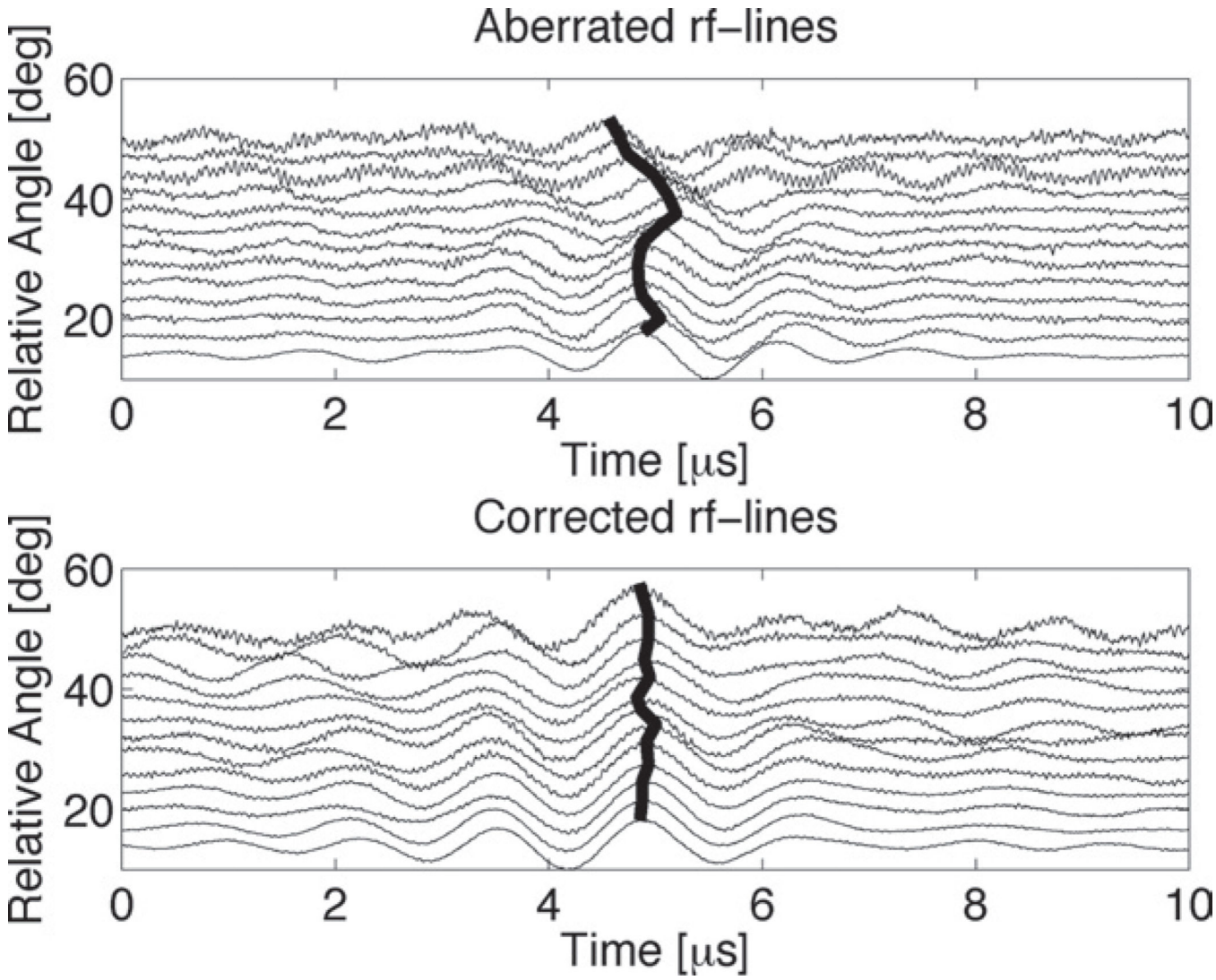


**Fig. (4).**

Ultrasound transcranial radiofrequency lines gathered using *ex vivo* human skulls. Misalignment of the peak amplitude of an ADV point beacon due to aberration (top) was corrected using time-reversal focusing (bottom). Reprinted from *Ultrasound in Medicine & Biology*, Vol. 34, Haworth KJ, Fowlkes JB, Carson PL, Kripfgans OD, "Towards aberration correction of transcranial ultrasound using acoustic droplet vaporization", 435–45 (2008), with permission from Elsevier.

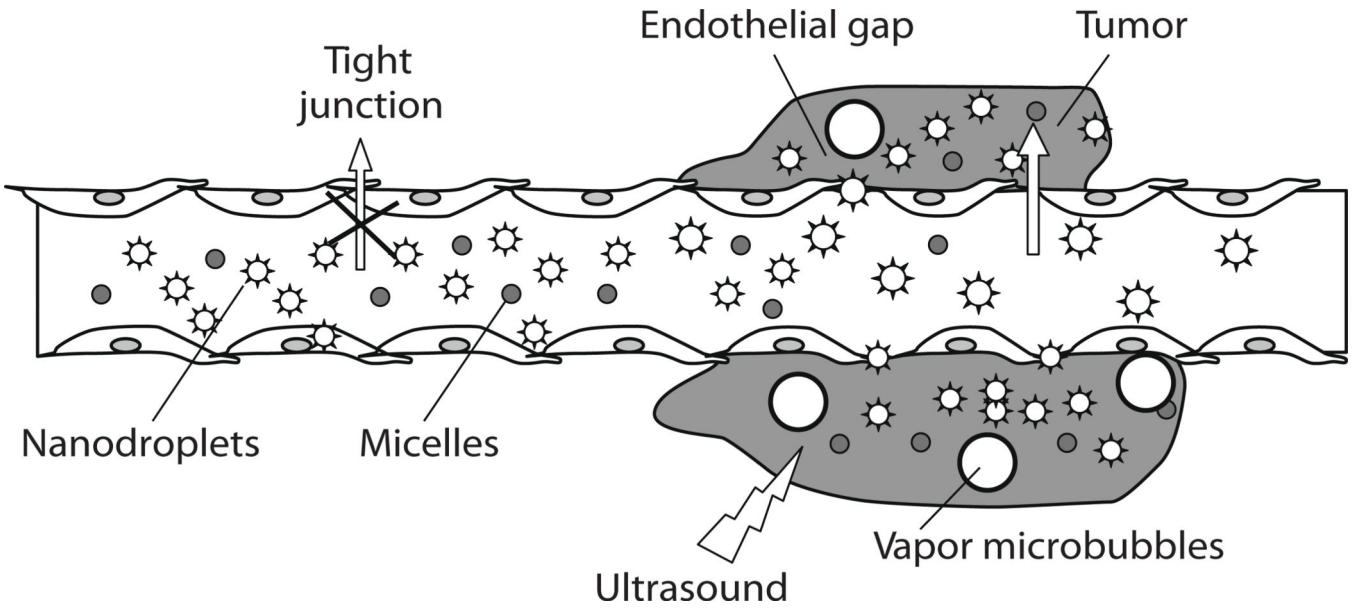


**Fig. (5).**

Schematic representation of passive drug targeting through the defective tumor microvasculature using an echogenic drug delivery system. The system comprises micelles (small circles), PFC nanodroplets (stars), and PFC microbubbles (large circles). Lipophilic drugs can be localized in the micelle cores and in the walls of nanodroplets/microbubbles. Tumors are characterized by defective vasculature with large gaps between the endothelial cells, which allows extravasation of drug-loaded micelles and small nanodroplets into the tumor interstitium. Primary microbubbles are formed from the vaporization of nanodroplets due to hyperthermia or ultrasound, and larger microbubbles appear due to coalescence of the primary microbubbles. Rapoport N, Gao Z, Kennedy A, “Multifunctional nanoparticles for combining ultrasonic tumor imaging and targeted chemotherapy”, *J Natl Cancer Inst*, 2007, Vol. 99, 1095–106, by permission of Oxford University Press.

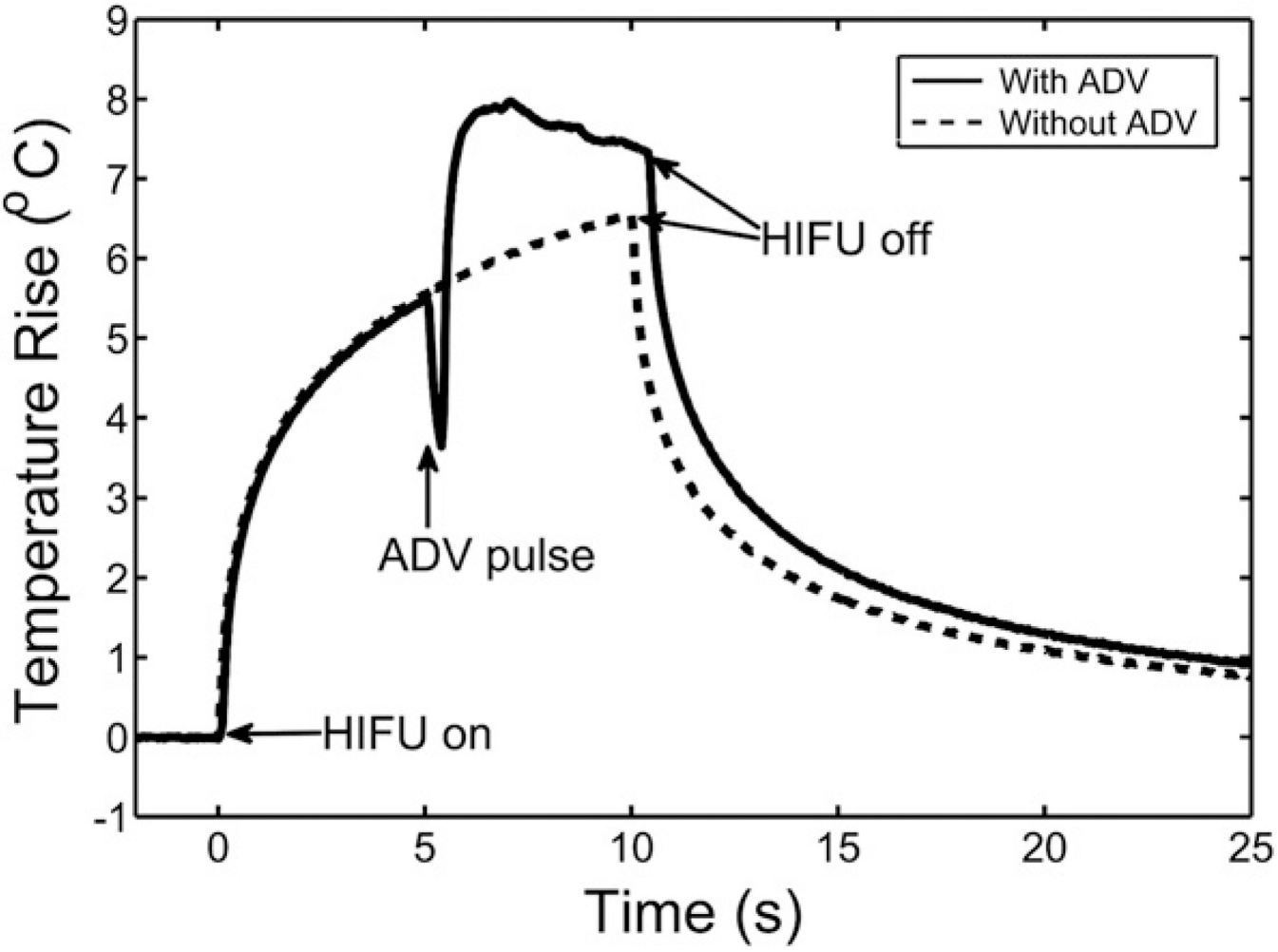


**Fig. (6).**

Presence of bubbles formed by vaporized DDFP nanodroplets increased the thermal delivery by ultrasound to a tissue-mimicking phantom. Temperature elevations were measured during a 10-second HIFU exposure with and without an ADV pulse. The function generator was switched from continuous to pulse mode to fire the ADV pulse, and then back to continuous mode for heat deposition. The switching period led to the temperature drop during that period of time. The measured temperature reached a plateau in the presence of vaporized nanodroplets, most likely because of shielding effects. Reprinted from *Ultrasound in Medicine & Biology*, Vol 36, Zhang P, Porter T, “An in vitro study of a phase-shift nanoemulsion: a potential nucleation agent for bubble-enhanced HIFU tumor ablation”, 1856–66 (2010), with permission from Elsevier.

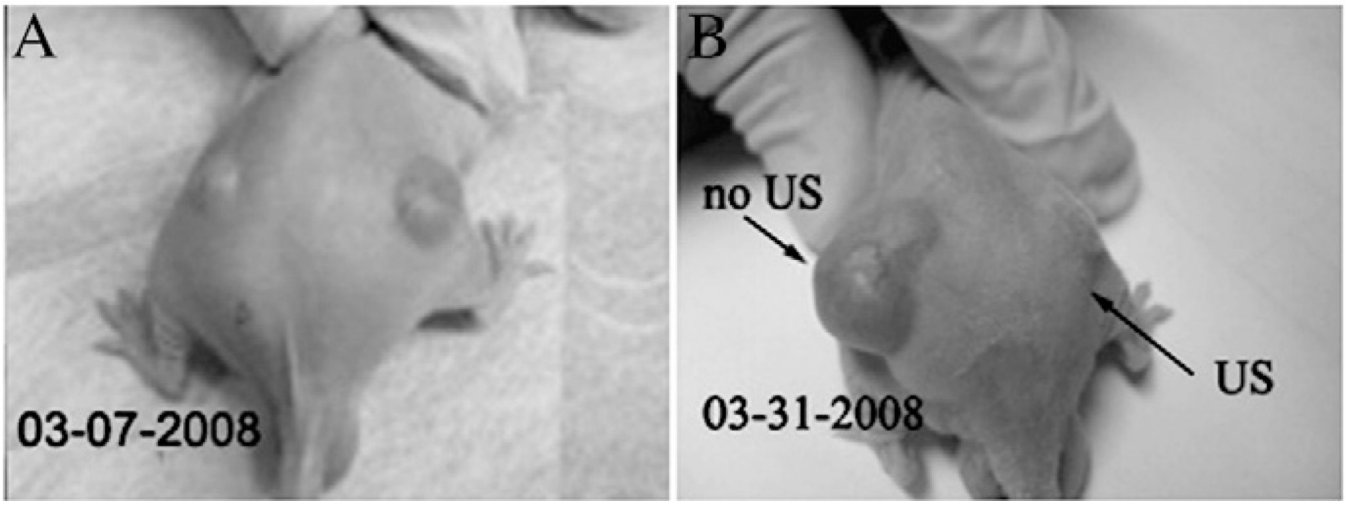


**Fig. (7).**

Demonstration of drug delivery by the interaction of ultrasound and drug-loaded nanodroplets/micelles. A nu/nu mouse bearing two ovarian carcinoma tumors immediately before (A) and 3 weeks after the treatment (B). The mouse was treated by four systemic injections of paclitaxel-loaded nanodroplets given twice weekly, while only the right tumor was sonicated by 1 MHz continuous-wave ultrasound 4 hours after the injection. The left tumor grew at the same rate as the controls, while the right tumor regressed, demonstrating paclitaxel release into the tumor volume. Reprinted from *J Control Release*, Vol. 138, Rapoport NY, Kennedy AM, Shea JE, Scaife CL, Nam KH, “Controlled and targeted tumor chemotherapy by ultrasound-activated nanoemulsions/microbubbles”, 268–76 (2009), with permission from Elsevier.

**Table 1**

Properties of Selected PFCs used for inert liquid emulsions, MCAs, and PCCAs

| PFC Name | Chemical Formula | Mol. Weight (g/mol) | Boiling Point (°C) | Surface Tension (mN/m) | Density ($kg/m^3$), 25°C | Phase Velocity (m/s), 25°C | CAS # |
|---|---|---|---|---|---|---|---|
| Perfluoro-octylbromide | $C_8F_{17}Br$ | 498.96 | 143 | 17.43 | 1930 | 631.8 | 423-55-2 |
| Perfluorodecalin | $C_{10}F_{18}$ | 462.08 | 140–143 | 19.41 | 1910 | 700.8 | 60433-11-6 |
| Perfluorooctane | $C_8F_{18}$ | 438.06 | 99 to 106 | 14.47 | 1730 | 579.4 | 307-34-6 |
| Perfluoro-methycyclohexane | $C_7F_{16}$ | 388.05 | 80 to 84 | 13.55 | 1680 | 586.1 | 335-57-9 |
| Perfluorohexane | $C_6F_{14}$ | 338.04 | 58 to 60 | 12.23 | 1680 | 520.9 | 355-42-0 |
| Dodecafluoro-pentane | $C_5F_{12}$ | 288.03 | 28 to 30 | 9.5 | 1590 | | 678-26-2 |
| Decafluorobutane * | $C_4F_{10}$ | 238.03 | −1.7 | | | | 355-25-9 |
| Octafluoropropane * | $C_3F_8$ | 188.02 | −36 to −39 | | | | 76-19-7 |

* indicates PFC exists in a gaseous state at 25°C

**Table 2**

Relation of Influencing Factors to US Vaporization Threshold

| **Environmental** | | |
|---|---|---|
| ***Factor*** | ***Relation to US Pressure Threshold*** | ***References*** |
| Ambient Temp. | Inverse | [72, 75, 76, 82, 83] |
| Ambient Pressure | Direct | Governing Eqs. |
| Viscosity of Surrounding Medium | Direct | [71, 75] |
| Presence of MCAs | Inverse | [74] |
| **Droplet Design** | | |
| ***Factor*** | ***Relation to US Pressure Threshold*** | ***References*** |
| PFC Boiling Point | Direct | [66, 73, 75, 84, 85] |
| Droplet Diameter | Inverse | [66, 75–77] |
| Shell Surface Tension | Direct | [53] |
| Incorporated Nanoparticles | Inverse | [85] |
| Droplet Concentration | No Effect or Inverse | [72, 83] |
| **Ultrasound Parameters** | | |
| ***Factor*** | ***Relation to US Pressure Threshold*** | ***References*** |
| Frequency | Inverse | [51, 71, 76] |
| Pulse Length | No Effect or Inverse | [72, 74–76, 83] |
| Pulse Repetition Frequency | No Effect or Inverse | [74, 75] |

## Table 3

*In vivo* PCCA studies

| Application | Animal | Target | Outcome | References |
|---|---|---|---|---|
| ***Embolotherapy*** | adult canine (mongrel) | externalized kidney | Up to 34% regional perfusion reduction in kidneys; Bubbles stationary for over 30 minutes; | [51] |
| | | kidney: non-externalized and externalized | Flow reduction in externalized and non-externalized kidneys; Instances of cardiac arrhythmia, respiratory distress, and death depending on injection type and dose | [90] |
| | New Zealand white rabbit | externalized kidney | Average organ perfusion reduction of >70%; Instances of pulmonary hyperinflation eliminated once droplets filtered | [88] |
| ***Aberration Correction*** | adult canine (mongrel) | brain exposed by bilateral craniotomy | Point beacons for aberration correction created; Significant increase over surrounding tissue | [51] |
| ***Cavitation Bioeffects, Gene Transfer*** | balb/c mice | subcutaneous RENCA tumor model | Enhanced cell transfection; Tumor growth rate reduction | [105] |
| | adult canine (mongrel) | liver | HIFU exposure in presence of droplets created 15-fold increase in lesion volume | [55] |
| ***Internal Markers*** | chicken embryo | various | Spatial control over release of fluorescent markers demonstrated | [108] |
| ***Drug Delivery*** | athymic nude mice | subcutaneous A2780 ovarian cancer and MB231 breast cancer models | Delivery of paclitaxel and doxorubicin resulted in substantial tumor growth rate reduction; Eventual tumor re-growth observed | [109] |
| | nu/nu mice | subcutaneous A2780 ovarian cancer and orthotopic MiaPaCa-2 pancreatic cancer models | Delivery of paclitaxel and doxorubicin resulted in substantial tumor growth rate reduction; Eventual tumor re-growth observed with exception of one instance of complete regression | [52–54, 81, 89] |
| ***Nanoparticle Delivery*** | SCID mice | hepatocellular carcinoma (HCC) tumor xenograft | Intra-tumoral vaporization of nanodroplets loaded with quantum dots | [85] |
| | New Zealand white rabbit | free circulation | Biodistribution of quantum dots obtained through histology | [85] |
| ***Diagnostic Imaging*** | SCID mice | hepatocellular carcinoma (HCC) tumor xenograft | Image contrast enhancement within mice hepatomas after droplet vaporization | [85] |
| ***$^{19}$F MR Co-Imaging*** | Swiss Webster white mice | free circulation | Nanodroplet pharmacokinetics measured | [54] |
| | nu/nu mice | orthotopic MiaPaCa-2 pancreatic cancer model | Preliminary biodistribution co-imaging with $^{19}$F MR demonstrated | [54] |